GEOPHYSICS, VOL. 66, NO. 5 (SEPTEMBER-OCTOBER 2001); P. 1457–1470, 10 FIGS., 8 TABLES.

Empirical estimation of viscoelastic seismic parameters from petrophysical properties of sandstone

Adam P. Koesoemadinata and George A. McMechan≥

ABSTRACT

Viscoelastic seismic parameters are expressions of underlying petrophysical properties. Theoretical and empirically derived petrophysical/seismic relations exist, but each is limited in the number and the range of values of the variables used. To provide a more comprehensive empirical model, we combined lab measurements from 18 published data sets and well log data for sandstone samples, and determined least-squares coefficients across them all. The dependent variables are the seismic parameters of bulk density (ϕ), compressional and shear wave velocities (V_p and V_s), and compressional and shear wave quality factors (Q_p and Q_s). The independent variables are effective pressure, porosity, clay content, water saturation, permeability, and frequency. As the derived expressions are empirical correlations, no causal relations should be inferred.

Prediction of ϕ is based on volumetric mixing of the constituents. For V_p and V_s predictions, separate sets of coefficients are fitted for three water saturation conditions: dry, partially saturated, and fully saturated. Predictions of V_p and V_s are fitted as functions of porosity, clay content, effective pressure, saturation, and frequency. Predictions of $100/Q_p$ are fitted as a function of porosity, clay content, permeability, saturation, frequency, and pressure. Interactions between effective pressure, saturation, and frequency are included. Predictions of $100/Q_s$ are obtained from Q_s/Q_p and $100/Q_p$.

The result is a composite model that is more comprehensive than previous models and that predicts seismic properties from the petrophysical properties. Empirically estimated values of ϕ, V_p, V_s, $100/Q_p$, and $100/Q_s$ for the composite data over all saturations predict the measurements with correlation coefficients (R^2) that range from a low of 0.65 (for $100/Q_s$) to a high of 0.90 (for V_p). As the fitted relations have been derived from data with limited parameter ranges, extrapolation is not advised, and they are not intended to substitute for locally derived relations based on site-specific data. Nevertheless, the derived expressions produce representative values that will be useful when approximate, internally consistent predictions are sufficient. Potential future applications include building of seismic reservoir models from petrophysical data and analysis of the sensitivity of seismic data to changes in reservoir properties.

INTRODUCTION

Detailed characterizations of aquifers and hydrocarbon reservoirs are important input for improving production strategies. Crosswell tomography, 3-D seismic reservoir imaging, and seismic inversion techniques can be useful to reservoir engineers only if the extracted seismic information can be translated into petrophysical information about the reservoir. Thus, there is a practical need for quantifying and understanding the relations between seismic parameters and petrophysical properties.

Empirical relations between the petrophysical variables [e.g., porosity (ϕ), clay content (C), effective permeability (k), water saturation (S_w), effective pressure (P_e), and frequency (f)] and the seismic parameters [compressional and shear velocities (V_p and V_s), compressional and shear quality factors (Q_p and Q_s), and bulk density (ϕ)] of sandstone samples have been the subject of many recent studies (Table 1). Other lithologies are less well studied, so we restrict our analysis to the sandstone data. Both theoretical models and laboratory measurements conclude that both seismic velocity and seismic attenuation in sandstone reservoirs correlate with the petrophysical properties. Previous studies rarely involved more than a couple of independent and dependent variables, so each provides data on only a subset of the whole suite of relevant interactions.

Manuscript received by the Editor November 29, 1999; revised manuscript received January 10, 2001.
≥The University of Texas at Dallas, Center for Lithospheric Studies, P. O. Box 830688, Richardson, Texas 75083-0688. E-mail: adam@utdallas.edu; mcmec@utdallas.edu.

In general, petrophysical and seismic parameters have trends with depth that reflect both increasing pressure and diagenetic changes. Scatter about these overall trends is associated with variations in texture, sorting, clay content, saturation, and so forth. These local changes may exhibit very different trends that are superimposed on the underlying depth-dependent variations and are crucial for mapping lateral changes within a reservoir. The viscoelastic responses of these microstructures are frequency dependent. Thus, it is important to include the environmental factors of pressure and frequency as well as rock microstructure data in predicting the viscoelastic properties.

The purpose of this study is to define empirical relationships between petrophysical properties and seismic parameters. By combining many data sets in which various petrophysical and seismic parameters were measured, we can obtain relations that involve more parameters than any of the individual studies did separately and thereby obtain a more comprehensive model. Although the previous studies are all to some degree incomplete, the measurements in them are the best available data, and so provide the data base for the current study.

The motivation for this development comes from the potential uses of the resulting empirical relations. The most direct application is in assignment of seismic properties to reservoir models that are defined in terms of their spatial distributions of petrophysical properties; this allows evaluation of the sensitivity of seismic responses to changes in petrophysical variables. It also provides a guide for petrophysical interpretation of seismic observations and sets the stage for explicit inversion [e.g., by amplitude variation with offset (AVO) analysis] for estimation of petrophysical information from seismic data. These applications are beyond the goals of the present study.

THE DATA BASE

Tables 1 and 2 show the sources, types, and ranges of values of the seismic and petrophysical (lab and well log) data that were used in model fitting. It is important to note that there are datasets that we didn't use. For example, we used density and V_p but not Q_p data from Shatilo et al. (1998) because, although the measurements appear to be reliable, the observed Q_p values were anomalously low, probably indicating the presence of an unusual attenuation mechanism. Also, empirical relationships from Castagna et al. (1985) for V_p and V_s as a function of porosity and clay content were used as examples, but not in the primary fitting, because they lacked explicit information on the ranges of porosity and clay content, the effective pressure, and the frequencies used. A few individual data points were also not used because they were beyond the defined constraints for the fitted equations. For example, we used only sandstone samples, to reduce lithologic effects. For the velocities, we included only samples of consolidated sandstone with volume fraction of clay $\geq$0.48, and for attenuation,

Table 1. Previous studies and data.[≤]

	V_p	V_s	ϕ	Q_p	Q_s	f	ϕ	C	P_e	S_w	k
Gregory (1976)	≥	≥	≥			≥	≥	≥	≥	≥	
Clark and Tittmann (1980)				≥	≥	≥	≥	≥	≥	≥	≥
Frisillo and Stewart (1980)				≥		≥	≥		≥	≥	≥
Murphy (1982)	≥	≥		≥	≥	≥	≥	≥	≥	≥	≥
Tosaya (1982)	≥	≥				≥	≥	≥	≥	≥	
Winkler and Nur (1982)	≥	≥		≥	≥	≥	≥	≥	≥	≥	≥
Jones and Nur (1983)		≥			≥	≥	≥	≥	≥	≥	≥
Murphy (1984)	≥	≥				≥	≥	≥	≥	≥	≥
Castagna et al. (1985)	≥	≥					≥	≥		≥	
Han et al.(1986)	≥	≥	≥				≥	≥	≥	≥	
Klimentos and McCann (1990)	≥			≥	≥	≥	≥	≥	≥	≥	≥
Miller and Stewart (1990)	≥	≥				≥	≥	≥	≥	≥	
Total-Indonesie (unpublished)	≥	≥	≥			≥	≥	≥	≥	≥	
Best et al. (1994)	≥	≥	≥	≥	≥	≥	≥	≥	≥	≥	≥
Tutuncu et al. (1994)			≥				≥	≥	≥	≥	
Best and McCann (1995)	≥	≥		≥		≥	≥	≥	≥	≥	
Jones (1995)	≥	≥				≥	≥	≥	≥	≥	
Tao et al. (1995)	≥	≥	≥	≥	≥	≥	≥	≥	≥	≥	≥
Shatilo at al. (1998)	≥		≥			≥	≥	≥	≥	≥	

[≤]V_p = P-wave velocity, V_s = S-wave velocity, ϕ = bulk density, Q_p = P-wave quality factor, Q_s = S-wave quality factor, f = frequency, ϕ = porosity, C = clay content, P_e = effective pressure, S_w = water saturation, and k = permeability. Units are defined in the text.

Table 2. Ranges of values for the data in Table 1 that were used in model fitting. Units are defined in the text.

Dependent variables	f	ϕ	C	P_e	S_w	k
V_p (km/s)	0.00056–1.0	0.02–0.35	0.0–0.48	0.1–68.9	0.0–1.0	N/A
V_s(km/s)	0.00038–1.0	0.02–0.30	0.0–0.48	0.1–68.9	0.0–1.0	N/A
V_p/V_s	0.00056–1.0	0.04–0.27	0.0–0.44	0.1–60.0	0.0–1.0	N/A
ϕ (g/cm^3)	N/A	0.03–0.306	0.0–0.44	3.6–40.0	0.0–1.0	N/A
Q_p	0.00046–1.0	0.027–0.36	0.0–0.29	0.1–60.0	0.0–1.0	0.0–1170.0
Q_s	0.00002–0.880	0.088–0.259	0.01–0.29	0.1–60.0	0.0–1.0	0.0–1170.0
Q_s/Q_p	0.00046–0.880	0.085–0.259	0.01–0.29	0.1–60.0	0.0–1.0	N/A

≥0.29 (Vernik, 1997). The intrinsic attenuation mechanisms in shale are expected to be different from those in sand (Shatilo et al., 1998; Stoll, 1981) and so are not expected to be fitted by the same models. Except for the density calculations, water is the only fluid explicitly considered. For velocity and Q predictions, it is assumed that air and natural gas have similar effects.

In the model fitting, the choice of parameters that were included was based on the concept that one should use all obvious parameters except when there is inconsistency within a data set (as indicated by a fitting error larger than the data values), or if there is explicit evidence that the parameter is not relevant, or if two or more petrophysical parameters appear not to be independent in their influence on the dependent seismic variable. We use all the seismic and petrophysical parameters for which reliable measurements are available (Tables 1 and 2), and employed the standard SAS software (release 6.12) for least-squares fitting of the functions.

Most of the lab measurements are on samples from the Gulf of Mexico or the adjacent North American continent. We also included data from two offshore wells (Peciko 9 and 10) in the Kutai Basin in East Kalimantan, Indonesia. The goal in including these well data was to provide broader applicability of the results (as they are lower frequencies than the lab measurements and are from a different sedimentological sequence). In the end, these well log data have slightly higher variance, but follow the same trends as the lab data.

The data used are only as complete as the studies from which they were obtained. Thus, we find that some variables that might be considered to be important are not included. These variables are generally less well understood, more difficult to measure, not independent of the variables that are in the model, or not available. Examples are pore aspect ratio, tortuosity, grain-size distribution, fluid viscosity, and temperature.

Before consideration of the fitted relations and the results, one final caution is in order. The relations obtained are correlations only; no causality should be implied (except for the special case of density, where the relation is clear). The separation into independent (petrophysical) and dependent (seismic) variables is determined by the defined goals of the study, and so is somewhat artificial. Some characteristics of the behavior of the data may be produced by interactions between the variables that are not considered. Nevertheless, the relations obtained do provide better, more comprehensive predictions (as indicated by the final correlation coefficients) than those previously available. The following sections consider fitting of each of the seismic/petrophysical relations in turn.

DENSITY MIXING EQUATION

Bulk rock density (ϕ_b) is defined by the density and volume fraction of each of the matrix and pore fluid constituents. Thus, density prediction is straightforward using the mixing ratio equation for composite media, and the only sources of uncertainties are in estimation of these two factors. While this is not an empirical equation, it is important to include it to indicate the uncertainties in density, as the same volume fraction data affect estimation of the other dependent variables. The mixing equation is

$$\phi_b = \sum_{i=1}^{n} \phi_i V_i, \qquad (1)$$

where ϕ_i and V_i are the density and volume fraction of the ith of the n components, respectively, and $\sum V_i = 1$. For the lab data in our study, the relevant constituents are quartz (with density 2.65 g/cm^3), clay (with density 2.6 g/cm^3), water/brine (with density 1.00/1.15 g/cm^3), oil (with density 0.854 g/cm^3 at 34.2≥ API), air (with density 0.00129 g/cm^3), and natural gas (with density 0.000717 g/cm^3). These values for the fluid components are at 14.7 psi and 25≥C (Gregory, 1976). For the well log data, there is no air, and we compute the density of natural gas (assumed to be methane) and brine as functions of temperature, pressure, and salinity as described by Batzle and Wang (1992).

Figure 1 contains a cross-plot between measured and predicted bulk densities across different saturation conditions and pressures (Table 2). The correlation coefficient R^2 is 0.86. If the well log data are excluded, R^2 is 0.95, because the well data have inherently higher measurement uncertainties. Equation (1) is valid only when ϕ_i and ϕ_b are measured at the same temperature and pressure.

VELOCITY—PETROPHYSICAL RELATIONS

In an elastic medium, V_p and V_s can be defined from the dynamic elastic constants and density. In a viscoelastic medium, the Lamé parameters ϕ and ϕ are pressure and frequency dependent, so velocities also become pressure and frequency dependent. Thus, approaches like the time-average equation introduced by Wyllie et al. (1956) and its improvement by Raymer et al. (1980) have limited applicability for viscoelastic materials.

Several theoretical models of elastic moduli have been proposed for composite media (e.g., Wood's equation, the Voight-Reuss-Hill model, Hashin-Shtrikman bounds, the Gassmann equation, Biot theory, the Kuster-Toksöz model, Hill's self-consistent model, Wu's self-consistent model, Korringa et al.'s model, ordered packing of spheres, Digby's model, Walton's model, and Brandt's equation). However, no theory has provided a good overall fit to data because assumptions must be made in any theory of elastic properties (or wave propagation) in effective media to make the mathematical models tractable (Wang and Nur, 1992).

Empirical approaches based on lab or log measurements seem to give qualitatively useful results. Experimental ultrasonic results (Tosaya, 1982; Kowalis et al., 1984; and Han et al., 1986) and measurements from well logs (Castagna et al., 1985) show that V_p and V_s in water-saturated sandstones and shales vary almost linearly with the porosity and the volume fraction of clay. Klimentos (1991) found the effect of permeability alone on V_p in rocks with identical porosity and clay content to be negligible.

Eberhart-Phillips et al. (1989), using data from Han et al. (1986), applied stepwise multiple regression to obtain least-squares best-fit predictions of velocities from porosity, clay content, and effective pressure. Their results show the pressure dependence among the samples does not correlate with porosity or clay content. Therefore, porosity, clay content, and effective pressure were treated as independent variables. The existence of velocity dispersion (Winkler, 1985, 1986; Jones, 1986; Sams et al., 1997) implies that frequency should be treated as a variable (in addition to other petrophysical variables), for velocity prediction. The general form of the relation used is

$$V(\mathrm{km/s}) = a_1 + a_2\phi + a_3 C + a_4 \ln(P_e) + a_5 S_w + a_6 f, \quad (2)$$

where a_1 to a_6 are the fitting coefficients for porosity (ϕ, in volume fraction), clay content (C, in volume fraction), the natural logarithm of effective pressure (P_e, in MPa), the water saturation (S_w, dimensionless fraction of pore space), and frequency (f in MHz). The intercept (a_1) implicitly contains the aggregate effects of all other possible parameters and parameter interactions that are not explicitly included. For V_p, the relations used are linear except for the logarithmic dependence on effective pressure and a frequency-saturation interaction at partial saturation (a_5 in Table 3).

Tables 3 and 4 contain the regression coefficients of equation (2) for V_p and V_s. For $S_w = 0.0$, both V_p and V_s appear to be independent of frequency, as previously suggested by Winkler (1985, 1986) and supported by experiments (Peselnick and Outerbridge, 1961; Spencer, 1981). Figures 2 and 3 contain cross-plots of the predicted and the measured V_p and V_s for the three saturation conditions. The values of R^2 for V_p are 0.69 for dry, 0.92 for partial saturation, and 0.82 for full saturation; for V_s, they are 0.68 for dry, 0.90 for partially saturation, and 0.78 for full saturation. To predict values in the gaps between the three saturation conditions, we interpolate linearly between the values computed from the coefficients given in Tables 3 and 4.

V_p/V_s ratios are also of interest as they are diagnostic of lithology (including degree of consolidation and water/gas saturation) (Gardner and Harris, 1968; Gregory, 1977; Bourbié et al., 1987). V_p/V_s ratios are predicted (Figure 4) using equation (2) but fitting the velocity ratio (rather than velocity) data. The V_p/V_s data set is considerably smaller that those for V_p and V_s, primarily because V_p and V_s were not often measured at the same saturations or frequencies. Table 5 contains the regression coefficients for V_p/V_s for $0.0 \geq S_w \geq 0.98$ and for $S_w = 1.0$. $R^2 = 0.68$ for the predicted/measured correlation over all saturations (Figure 4). When V_p/V_s is predicted from separately calculated V_p and V_s values, R^2 reduces slightly to 0.62.

Although the data of Castagna et al. (1985) were missing some explicit auxiliary information (see Introduction, above) and so were not included in the regressions, approximate values of the missing parameters could be inferred from the descriptions of the data acquisition. The corresponding estimates for V_p and V_s (assuming $P_e = 55.3$ MPa and $f = 0.015$ MHz) are

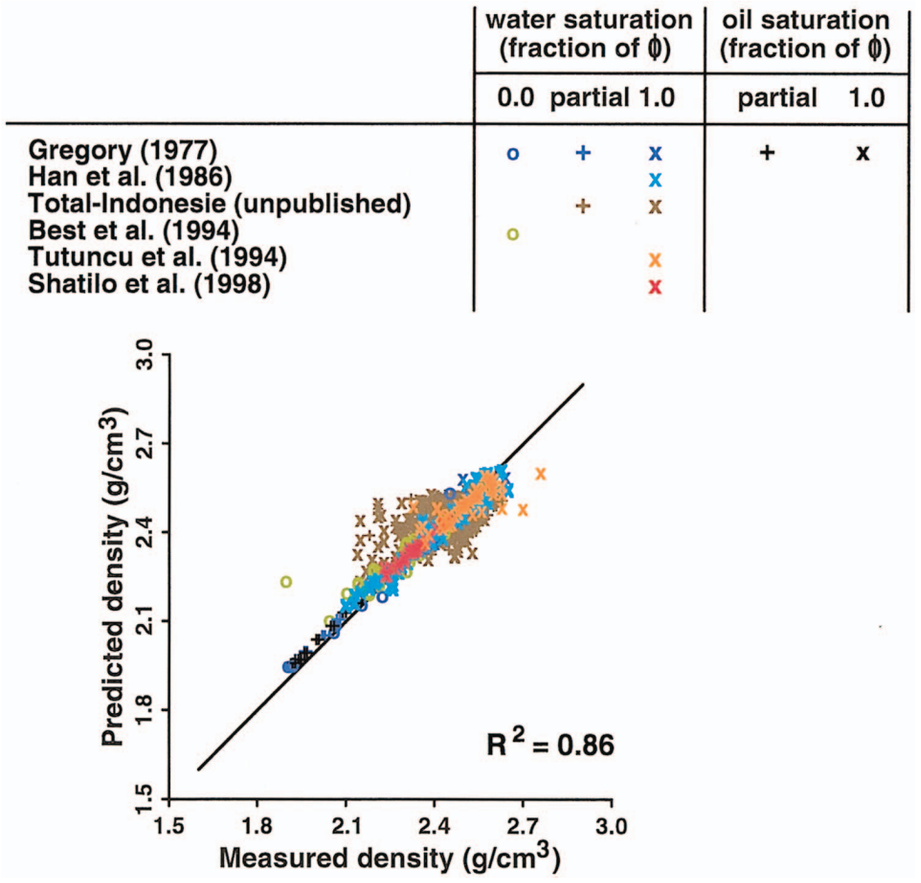

FIG. 1. Cross-plot of measured and the predicted bulk densities. The Total-Indonesie data are from unpublished well logs; all the rest are lab data. The "water saturation" column refers to samples whose pores contain the indicated water saturation; the remainder of the pore space of the lab samples is filled with air, and the remainder of the pore space near the wells is filled with natural gas. The "oil saturation" column refers to samples whose pores contain the indicated oil saturation; the remainder of the pore space is filled with air.

plotted in Figures 2c and 3c; the "measured" data are evaluations of Castagna's (1985) regression equations for $C = 0.15$ and $0.01 \geq \phi \geq 0.30$. These approximate predictions are consistent with the range of scatter of the other data predictions.

ATTENUATION—PETROPHYSICAL RELATIONS

The prediction of attenuation is more complicated than for velocities. Interaction of petrophysical properties (e.g., frequency and saturation) and the probable coexistence of more than one attenuation mechanism has the potential to significantly affect the observed attenuation behavior (Toksöz and Johnston, 1981). Attenuation depends on the product of frequency and pore fluid viscosity in the form of a Zener/Debye function that gives peak attenuation at certain relaxation frequencies (Jones, 1986) that depend on the scale of the physical mechanism involved. The amplitude and shape of the peak depend on saturation (Jones, 1986; Sams et al., 1997). Murphy (1982), Spencer (1979), and Klimentos (1995) also show that attenuation is strongly dependent on saturation, which makes the measurement and understanding of attenuation important for reservoir characterization (Toksöz and Johnston, 1981). At the low temperatures involved in lab measurements, the effect of temperature on the viscosity of water (e.g., Jones and Nur, 1983) is neglected, as we used only data from room temperature measurements. For dry rocks, attenuation is generally temperature-independent at $<150^{\circ}$C (Johnston, 1981).

Klimentos and McCann (1990) showed a linear relationship between P-wave attenuation and porosity and clay content. Best et al. (1994) showed that the quality factors of P-waves (Q_p) and S-waves (Q_s) depend on porosity and intrapore minerals (whether they are clays or carbonates). Shatilo et al. (1998) showed a strong correlation between P-wave attenuation and porosity, but no correlation between attenuation and clay content. For convenience, these studies fitted linear functions, but the variance is high. Thus, other functional relations can also be easily justified; we fit $100/Q$ rather than Q.

Both Q_p and Q_s values increase exponentially with increasing effective pressure at all saturations from dry to full (e.g., Winkler and Nur, 1979, 1982; Tao et al., 1995). These data also show that the effect of pressure on attenuation varies with water saturation and frequency; the pressure dependence is less in dry rocks (Winkler and Nur, 1979). These are complicated interactions that change as the attenuation mechanisms change with saturation and frequency. Hence, the pressure effect can not be treated independently of saturation and frequency.

Klimentos and McCann (1990), Akbar et al. (1993), and Shatilo et al. (1998) investigated the effect of permeability on Q_p. The results are inconclusive at best; the data have high variance suggesting that permeability is not a significant variable. The Klimentos and McCann (1990) data show attenuation decreasing with increasing permeability, but their final equations only include porosity and clay content. They suggested that attenuation is related to permeability in a complex way. Akbar et al. (1993), using a squirt flow model, found that attenuation decreases with increasing permeability and depends on the direction of wave propagation relative to the pore orientation. On the other hand, Shatilo et al. (1998), using sandstone with low ($\geq$0.16) clay content, showed attenuation (in water-saturated sandstone) increasing with increasing porosity and permeability, and suggested the relation between attenuation and rock properties may be environment dependent. Our results, described below, show that for clay content $\geq$0.29, permeability significantly affects attenuation.

Table 3. Least-squares regression coefficients of equation (2) for V_p.[≤]

S_w (fraction of ϕ)	a_1	a_2	a_3	a_4	a_5	a_6
0.00	3.661 (0.096)	≥5.552 (0.429)	≥0.689 (0.377)	0.364 (0.024)	—	—
0.02–0.98	4.492 (0.071)	≥10.994 (0.266)	≥1.138 (0.285)	0.211 (0.010)	$(15.2f - 15.0f^{1.1}) \geq 0.02$	0.423 (0.077)
1.00	4.705 (0.042)	≥7.155 (0.120)	≥2.140 (0.066)	0.164 (0.009)	—	0.338 (0.020)

[≥]V_p for $0.0 < S_w < 0.02$ and for $0.98 < S_w < 1.0$ are obtained by linear interpolation. Values in brackets are the associated standard errors. A dash (—) indicates that the corresponding variable is not significant, and so was not included in the fitting.

Table 4. Least-squares regression coefficients of equation (2) for V_s.[≤]

S_w (fraction of ϕ)	a_1	a_2	a_3	a_4	a_5	a_6
0.00	2.422 (0.061)	≥3.718 (0.280)	≥0.781 (0.241)	0.235 (0.015)	—	—
0.02–0.98	3.128 (0.043)	≥7.341 (0.145)	≥1.472 (0.159)	0.121 (0.007)	≥0.230 (0.043)	0.263 (0.045)
1.00	2.664 (0.034)	≥5.039 (0.114)	≥1.691 (0.062)	0.169 (0.007)	—	0.368 (0.024)

[≥]V_s for $0.0 < S_w < 0.02$ and for $0.98 < S_w < 1.0$ are obtained by linear interpolation. Values in brackets are the associated standard errors. A dash (—) indicates that the corresponding variable is not significant, and so was not included in the fitting.

Prediction of $100/Q_p$

Guided by the results of the previous studies, we use a relation between $100/Q_p$ and petrophysical properties of the form

$$100/Q_p = b_1 + b_2\phi + b_3 C + b_4 \ln(k) + b_5(S_w, f) \geq b_6(P_e, S_w, f), \quad (3)$$

where b_1, b_2, b_3, and b_4 are (least-squares) fitted coefficients (Table 6). Symbols ϕ, P_e, f, and S_w are defined above, and k is permeability (in millidarcys). Coefficient b_5, shown in Figure 5, is based on room pressure data from Murphy (1982, 1984) and Frisillo and Stewart (1980), corrected to compensate for differences in porosity, clay content, and permeability. Then, to incorporate the pressure dependence (b_6), all available data (Table 1) within the ranges shown in Table 2, were fitted to produce the pressure-frequency distributions contoured in Figure 6 for dry, full saturation, and the locus of peak attenuation. The latter is the heavy dashed line A-B in the saturation-frequency plane in Figure 5. Values of b_6 for other saturations are determined by nonlinear interpolation between the three reference saturation conditions, guided by the behavior in Figure 6.

Relation (3) may produce unrealistically low (even negative) values of $100/Q_p$, especially where there is coincidence of more than one of high pressure, low frequency, low saturation, and low porosity, as the data do not provide adequate constraints in these regions. To partially overcome this limitation, the maximum Q_p at any frequency is bounded by the observed empirical relation between V_p and Q_p for $S_w = 0.0$ (which we assume approximates the maximum possible Q_p; subjectively, tests show that this works well). Relationships between velocity and attenuation, for certain frequency ranges, have been shown in previous studies (e.g. Spencer, 1981; Martinez, 1992; Best et al., 1994). For dry rocks, we use the form

$$(100/Q_p)_{\min} = a(f)e^{\geq 1.4 V_p}, \quad (4a)$$

with

$$a(f) = 6.819 + 247.4f, \quad (4b)$$

where $(100/Q_p)_{\min}$ is the minimum bound of $100/Q_p$ as a function of V_p (Figure 7), $a(f)$ is a frequency-dependent coefficient, and f is frequency in MHz.

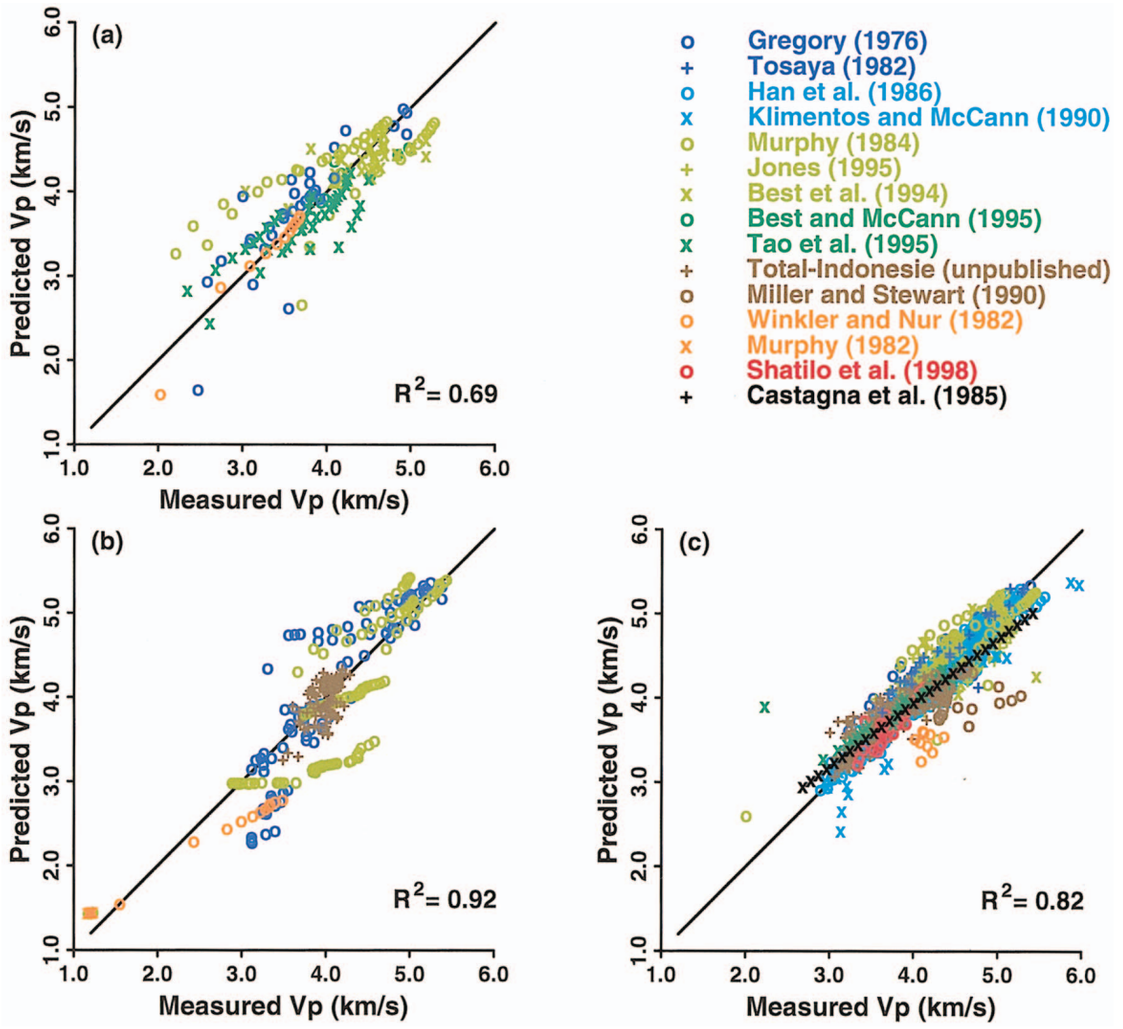

FIG. 2. Cross-plots of measured and predicted V_p for (a) $S_w = 0.0$, (b) $S_w = 0.02$–0.98, and (c) $S_w = 1.0$.

Representative predictions of $100/Q_p$ using equations (3), and (4), with the coefficients given in Table 6, are shown in Figure 8. The cross-plots of measured and predicted $100/Q_p$ have a composite $R^2 = 0.88$ for all petrophysical conditions considered.

Prediction of Q_s/Q_p and $100/Q_s$

Predictions of Q_s were guided by the conclusion of Murphy (1982) and Winkler and Nur (1982) that the Q_s/Q_p ratio is a sensitive indicator of partial saturation. Our analysis shows that the Q_s/Q_p function of saturation observed by Murphy (1982) is also dependent on other factors. To investigate these relationships between Q_s/Q_p and other properties, we did regression analyses in five zones of saturation and frequency. These are referenced to the locus of peak Q_p shown in Figure 5 as line A-B. The general form of the fitted relations is

$$Q_s/Q_p = c_1 + c_2\phi + c_3 \ln(C \geq 10^2) + c_4 \ln(P_e) + c_5 S_w + c_6 \log_{10}(f \geq 10^6), \quad (5)$$

where c_1 through c_6 are (least-squares) fitted coefficients (Table 7). This allows approximate prediction of Q_s from Q_p (or vice versa) using the predicted Q_s/Q_p ratio. For $0.001 < S_w < S_{w,PA} \geq 0.1$, there was an insufficient range of porosity data, and we assumed that the porosity coefficient (2.104) was the same as that found for $S_{w,PA} < S_w \geq 1.0$. This is consistent with the overall result that Q_s/Q_p depends on f at all S_w and becomes independent of S_w and ϕ at low S_w. P_e is more important at low S_w than at high S_w. C is important only at high f and low S_w.

Cross-plots of calculated and measured Q_s/Q_p are shown in Figure 9; $R^2 = 0.72$. Q_s/Q_p ratios are diagnostic of saturation (Winker and Nur, 1979; Bourbié et al., 1987), with lower Q_s/Q_p at full saturation than when dry or partially saturated. Figure 10 contains cross-plots of calculated and measured $100/Q_s$; $R^2 = 0.65$.

DISCUSSION

We have developed empirical relationships between petrophysical properties and seismic parameters using all the

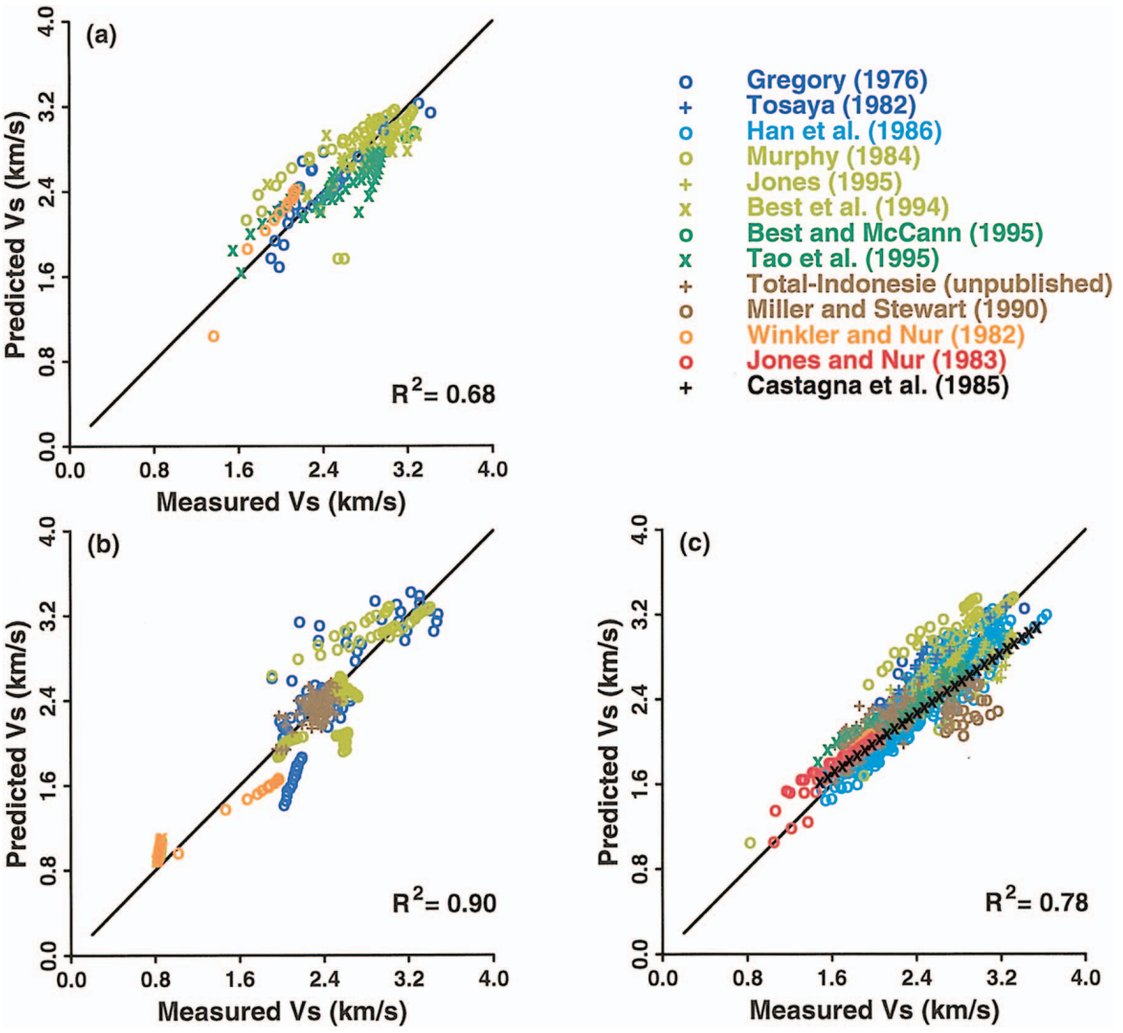

FIG. 3. Cross-plots of measured and predicted V_s for (a) $S_w = 0.0$, (b) $S_w = 0.02$–0.98, and (c) $S_w = 1.0$.

apparently relevant parameters and available measurements. Linear terms for the effects of porosity, clay content, and frequency, with an exponential term for the effect of pressure and a nonlinear interaction between saturation and frequency, appear to be adequate for predicting velocities. For attenuation, linear coefficients are obtained for porosity, clay content, and ln (permeability); effects of saturation, frequency, and pressure are included via interpolation in 2-D distributions. For better predictions over wider parameter ranges, other potentially salient factors include lithologic effects (e.g., quartz/feldpar ratios), pore aspect ratio, tortuosity, grain-size distribution, and the presence of cement (Shatilo et al. 1998). Neglect of these and of the unknown interactions between variables and processes, along with the arbitrary choice of the functions used to fit the relationships between variables, are the main expected sources of the remaining misfits. There is also no reason to expect that a single universal model exists for all sandstones.

In consolidated sandstone, with full water saturation at fixed pressure and frequency, V_p and V_s are mainly controlled by porosity and clay content. Other parameters such as pore geometry, grain size, grain contact morphology, cementation, type of clay, distribution of clays, and mineralogy have much less influence on velocities at high effective pressure (Han et al., 1986). At low effective pressures, V_p and V_s are sensitive to pore geometry and aspect ratio, as pores and cracks change shape with pressure; these changes decrease at large pressures where the cracks have closed.

Velocity data show a dependence on (partial) water saturation that changes with frequency, as there is a scale-dependence of the contribution of factors such as the interaction between gas and water, and local fluid flow to the effective dynamic elastic moduli (Gassmann, 1951; Murphy et al., 1993; Gist, 1994). The frequency-saturation term a_5 in equation (2) for V_p (Table 3) describes this behavior. Gregory (1976), using ultrasonic data, also observed a variation of velocity with saturation, depending upon composition (e.g., intergranular cement) and porosity; the effect of fluid saturation on velocity is larger in low porosity rock. Han et al. (1986) suggested that water saturation affects the velocities in sandstones as a

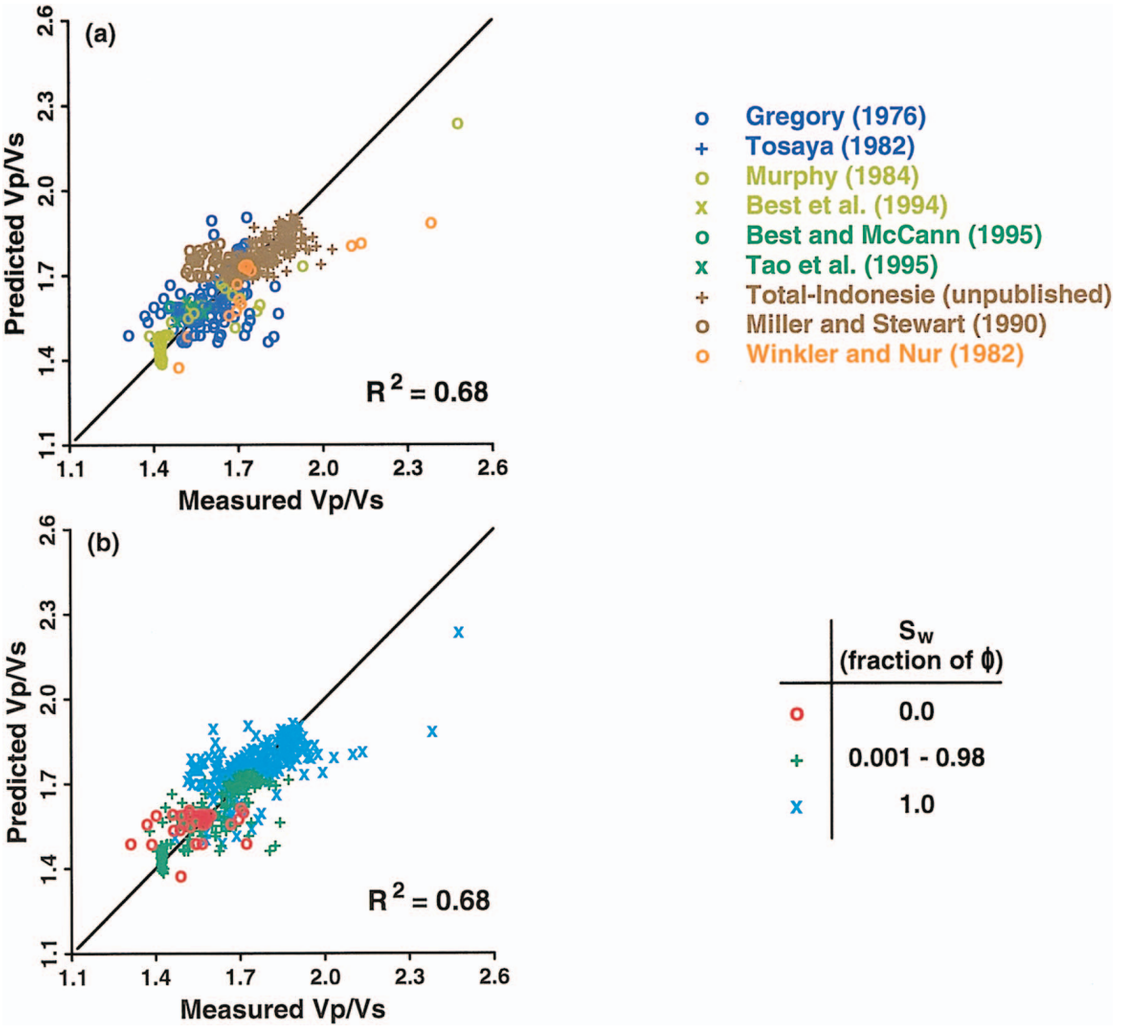

FIG. 4. Cross-plots of measured and predicted V_p/V_s. Predictions of V_p/V_s are obtained by fitting observed ratios using equation (2). In (a), symbols and colors show the sources of the data; in (b), colors show the ranges of saturation.

function of degree of consolidation, via interactions between the pore fluid (water) and clays; samples with the same porosity and clay content may have different degrees of consolidation which results in a variation in velocities. Presumably, the saturation-frequency parameter a_5 in equation (2) should also be porosity dependent, and this is a subject for further study. The good fit ($R^2 \geq 0.90$) between the measured and predicted velocities (Figures 2 and 3) shows that the relationships for partial saturation are generally reliable.

The effects of petrophysical parameters on attenuation are complicated and cannot be explained by a single model/mechanism for all lithologies and frequencies (Toksöz and Johnston, 1981). For example, different attenuation mechanisms of sandstone for clay $\geq$0.3 and $\geq$0.35 (Stoll, 1981; Shatilo et al., 1998) would require different models (which is why we considered only samples with low clay content).

One variable that was not explicitly considered is temperature. In dry rock or rock saturated with water or light hydrocarbons, velocities generally decrease 1–9% as temperature increases by 100≥C, but when the rock is saturated with heavy hydrocarbons, V_p decreases 10–35% as temperature increases by 100≥C (Wang and Nur, 1988). In the present context, we consider temperature effects to be implicitly included through their effects on the parameters that were explicitly used.

In general, the attenuations measured from small volumes (lab samples or logs) will underestimate the total in-situ attenuation as scale-dependent effects, caused for example by fracturing or by scattering by heterogeneties, are not included.

Table 6. Least-squares regression coefficients of equation (3) for $100/Q_p$. Values in brackets are the associated standard errors.

S_w (fraction of ϕ)	b_1	b_2	b_3	b_4
0.00–1.00	$\geq$2.540 (0.246)	18.497 (1.475)	3.715 (1.347)	$\geq$0.157 (0.033)

Table 5. Least-squares regression coefficients of equation (2) for V_p/V_s for $0.0 \leq S_w \leq 0.98$ and for $S_w = 1.0$.≤

S_w (fraction of ϕ)	a_1	a_2	a_3	a_4	a_5	a_6
0.0–0.98	1.480 (0.012)	—	—	0.044 (0.002)	0.118 (0.016)	$\geq$0.071 (0.011)
1.00	1.778 (0.046)	1.193 (0.133)	0.394 (0.063)	$\geq$0.073 (0.010)	—	$\geq$0.093 (0.019)

≥ V_p/V_s for $0.98 < S_w < 1.0$ is obtained by interpolation between 0.98 and 1.0. Values in brackets are the associated standard errors.

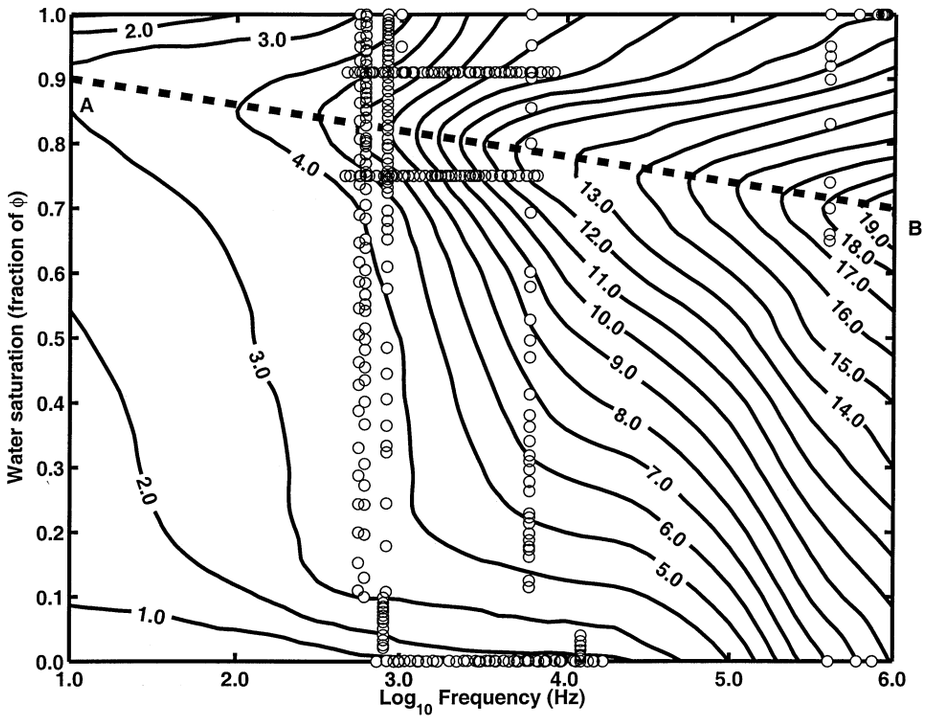

FIG. 5. Contours of $b_5(S_w, f)$ in equation (3) as a function of water saturation and frequency at room pressure. The dashed line A-B is the peak-attenuation trend; o symbols show the locations of the data points.

Only the intrinsic Q component is represented in the measurements used above.

The derived empirical relations for velocity prediction did not consider parameter interactions (except for frequency and saturation), so more work can yet be done. For example, it is interesting that the fitted relations cover all measurements for all conditions, but individual samples do not necessarily follow the best-fit equations. This is especially obvious in the V_p and V_s predictions at full saturation (Figures 2c and 3c), where individual sample trajectories can be seen cutting obliquely through the fitted data; this suggests that the form of the equation used for some parameter is not optimal (i.e., should be nonlinear), or that some salient parameter or interaction is missing from the parameterization. We do not expect an empirical model to be accurate for any specific sample. It is also true that we do expect the slope of each individual sample trajectory (in the predicted versus observed plot for all fitted parameters) to be less than the optimal 45≥ trend because the range of predicted values for any sample is necessarily less than that of the observed data.

Unlike velocity, which is often considered to be unaffected by permeability (Klimentos, 1991), attenuation has a significant correlation with permeability (Table 5). The relationship between attenuation and permeability is complicated (Klimentos and McCann, 1990; Akbar et al., 1993). Permeability is not independent of porosity (e.g. Bourbié et al., 1987; Schön, 1995); they correlate with each other, but they appear to generate physically different attenuation mechanisms.

From the relationships presented above, various auxiliary studies can proceed, such as the variation in V_p/V_s and Q_s/Q_p ratios with pressure and frequency. These are of particular importance in distinguishing gas from water sands (e.g., Murphy, 1982; Winkler and Nur, 1982; Klimentos, 1995). The defined relationships can also be used as a basis for generating realistic reservoir models for viscoelastic seismic modeling and AVO studies. The relations, their coefficients, and the form of the equations can be updated as new data become available. In addition, a similar approach can be used to produce empirical models for other lithologies, such as shales and carbonates.

One of the main concerns regarding the results obtained is that the ranges of many parameters in the data base are relatively small, so it is not clear (and not testable with existing data) how far the fitted equations may be reliably extrapolated. The fitted expressions are necessarily biased toward the specific data that were input. When using the expressions, the reader is

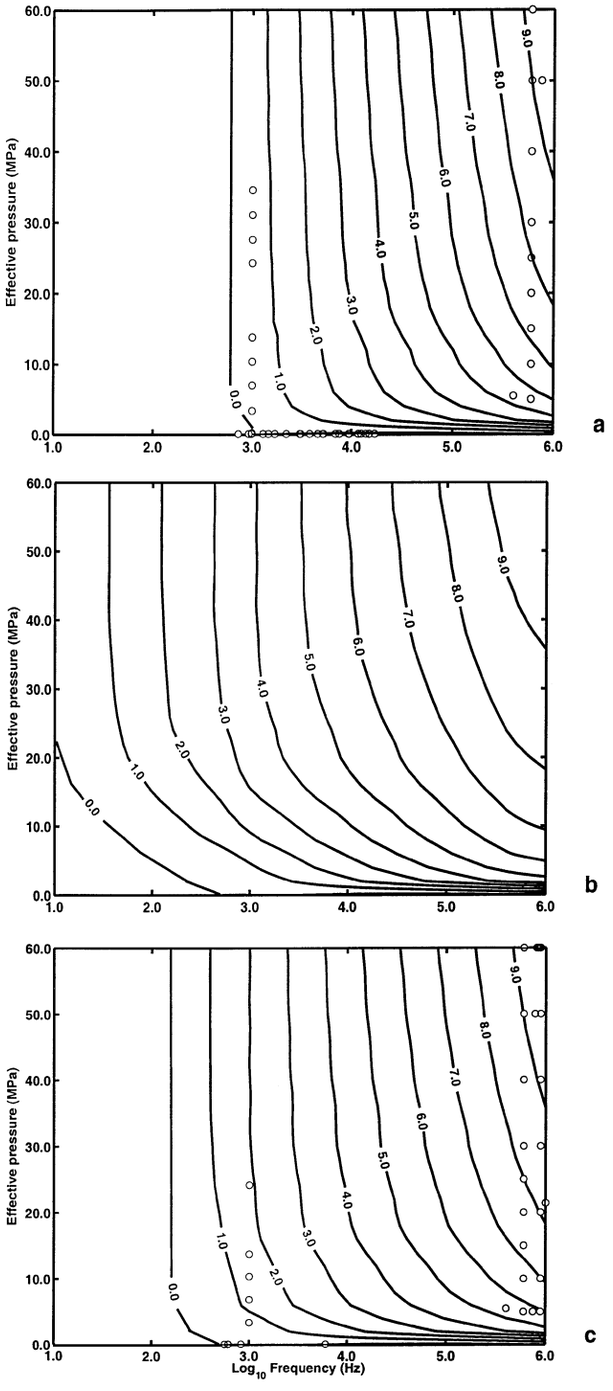

FIG. 6. Contours of $b_6(P_e, S_w, f)$ in equation (3) as a function of effective pressure and frequency: (a) is for dry samples, (b) is for the locus of peak Q_p (the line A-B in Figure 5), and (c) is for full saturation; o symbols show the locations of the data points.

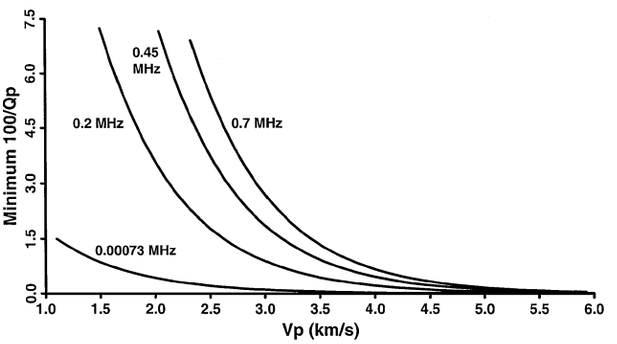

FIG. 7. Minimum values of $100/Q_p$ as a function of V_p and frequency. These lines, which are given by equation (4), are obtained by fitting bounds to all the data in Table 1 above 0.00073 MHz and above 0.7 MHz and interpolating for intermediate frequencies.

advised to refer to Table 2 and not to overextend predictions beyond the parameter ranges from which they were derived; in our own software, we have checkpoints that require a user override to make predictions beyond the defined bounds of the data. Table 8 contains the correlation coefficients and standard deviations for all the correlations in this paper to summarize the quality of the fits.

Finally, the reader must be cautioned regarding the applicability and use of the results. The results are all empirical; the equations describe correlations between seismic and petrophysical variables, but causality should not be inferred. In all situations, it is better to use relations derived locally from the specific lithologies and environments of interest, rather than the approximate, generalized expressions presented above, as the former will produce more accurate predictions of properties. However, when no local data are available, our results can be used to generate approximate seismic models.

SUMMARY

By combining many published data sets in which various petrophysical and seismic parameters were measured, we have obtained relations that involve more parameters than any of the individual studies did separately. The main petrophysical parameters accounting for velocities are effective pressure, frequency, porosity, clay content, and saturation. These parameters, in addition to permeability, are used to predict Q_p for clay content $\geq$0.29. Predictions of Q_s were made by using the Q_s/Q_p ratio as a function of saturation and frequency with the calculated Q_p. Table 8 contains a summary of the correlation coefficients of the V_p, V_s, ϕ, $100/Q_p$, and $100/Q_s$ predictions; R^2 for the composite predictions (for $0.0 \geq S_w \geq 1.0$) ranges from 0.65 to 0.90. The predicted Q values should be considered as the intrinsic Q component only.

It is clear that the best way to proceed with a further understanding of the effect of petrophysical properties on seismic

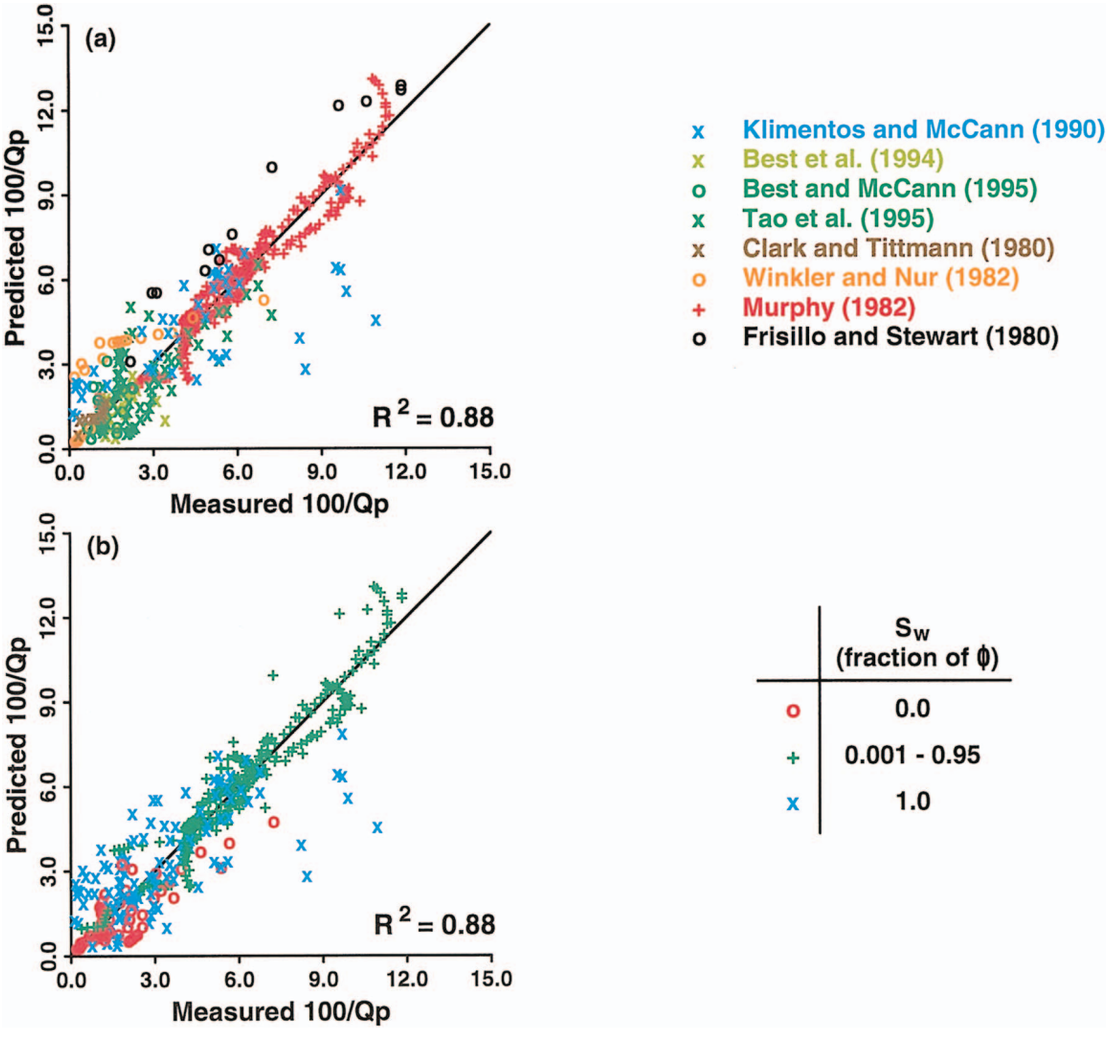

FIG. 8. Cross-plots of measured and predicted $100/Q_p$ [via equations (3) and (4), with the coefficients in Table 6]. In (a), symbols and colors show the sources of the data. In (b), symbols and colors show the ranges of saturation.

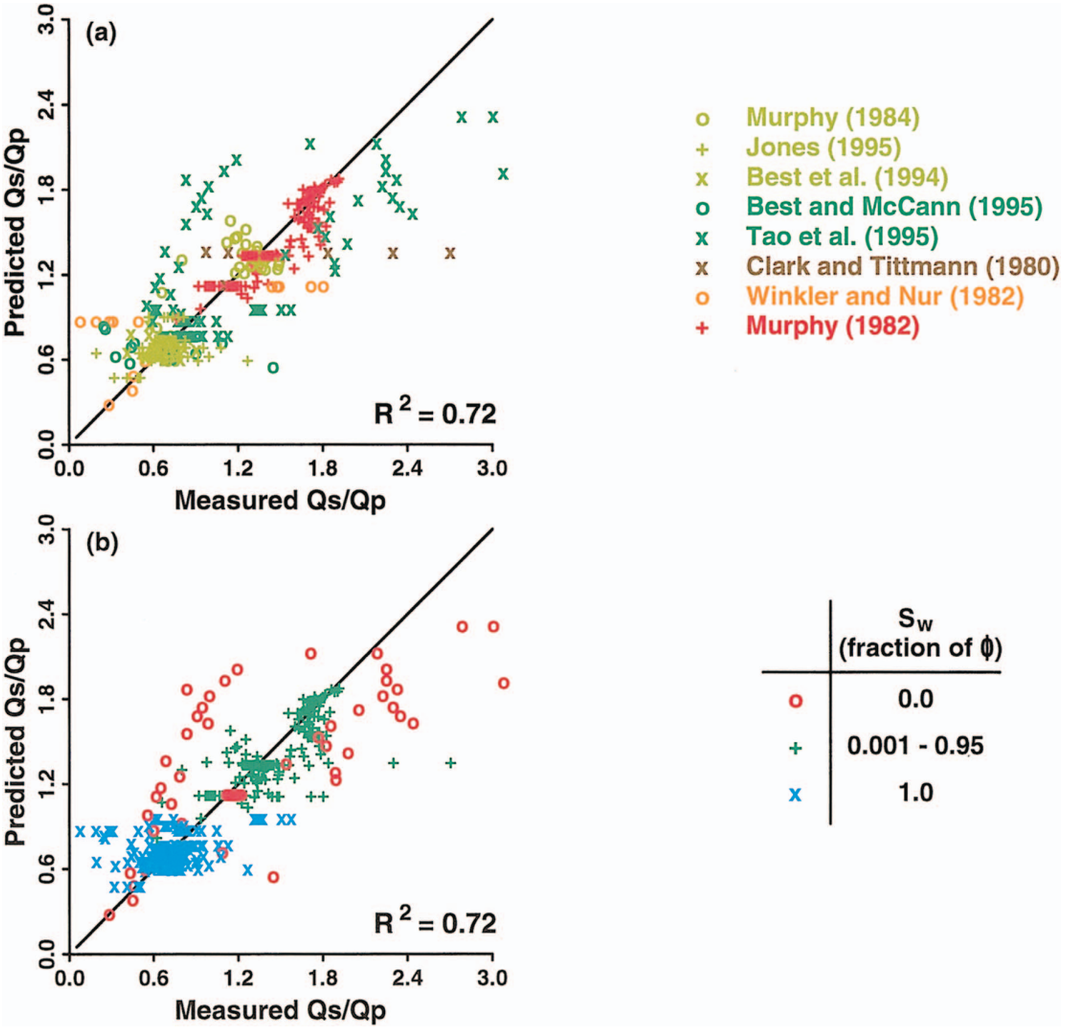

FIG. 9. Cross-plots of measured and predicted Q_s/Q_p [via equation (5)]. In (a), symbols and colors show the sources of the data. In (b), symbols and colors show the ranges of saturation.

parameters is to make comprehensive measurements of all independent and dependent variables on a large number of samples so the data are truly consistent.

ACKNOWLEDGMENTS

The research leading to this paper was supported by the sponsors of the Petroleum Research Fund of the American Chemical Society under grant 32721-AC2 and by the sponsors of the UTD Geophysical Consortium. The Peciko well data were kindly provided by Total Indonesie and Pertamina, Indonesia. Constructive comments by Gary Mavko and two anonymous reviewers improved the paper and are much appreciated. This paper is Contribution No. 934 from the Geosciences Department at the University of Texas at Dallas.

REFERENCES

Akbar, N., Dvorkin J., and Nur, A., 1993, Relating *P*-wave attenuation to permeability: Geophysics, **58**, 20–29.
Batzle, M., and Wang, Z., 1992, Seismic properties of pore fluids: Geophysics, **57**, 1396–1408.
Best, A. I., and McCann, C., 1995, Seismic attenuation and pore fluid viscosity in clay-rich reservoir sandstones: Geophysics, **60**, 1386–1397.
Best, A. I., McCann, C., and Southcott, J., 1994, The relationships between the velocities, attenuations and petrophysical properties of reservoir sedimentary rocks: Geophys. Prosp., **42**, 151–178.
Bourbié, T., Coussy, O., and Zinszner, B., 1987, Acoustics of porous media: Gulf Publ. Co.
Castagna, J. P., Batzle, M. L., and Eastwood, R. L., 1985, Relationships between compressional-wave and shear-wave velocities in clastic silicate rocks: Geophysics, **50**, 571–581.
Clark, V. A., and Tittmann, B. R., 1980, Effect of volatiles on attenuation ($Q^{\geq 1}$) and velocity in sedimentary rocks: J. Geophys. Res., **85**, 5190–5198.
Eberhart-Phillips, D. M., Han, D. H., and Zoback, M.D., 1989, Empirical relationships among seismic velocity, effective pressure, porosity and clay content in sandstone: Geophysics, **54**, 82–89.
Frisillo, A. L., and Stewart, T. T., 1980, Effect of partial gas/brine saturation on ultrasonic absorption in sandstone: J. Geophys. Res., **85**, 5209–5211.
Gardner, G. H. F., and Harris, M. H., 1968, Velocity and attenuation of elastic waves in sands: 9th Logging Symposium Trans., Soc. Prof. Well Log Analysts, M1–M19.
Gassmann, F., 1951, Uber die elastizität poröser medien: Vierteljahrsschrift der Naturforschenden Gesellschaft in Zurich, **96**, 1–23.
Gist, G. A., 1994, Interpreting laboratory velocity measurements in partially gas-saturated rocks: Geophysics, **59**, 1100– 1109.

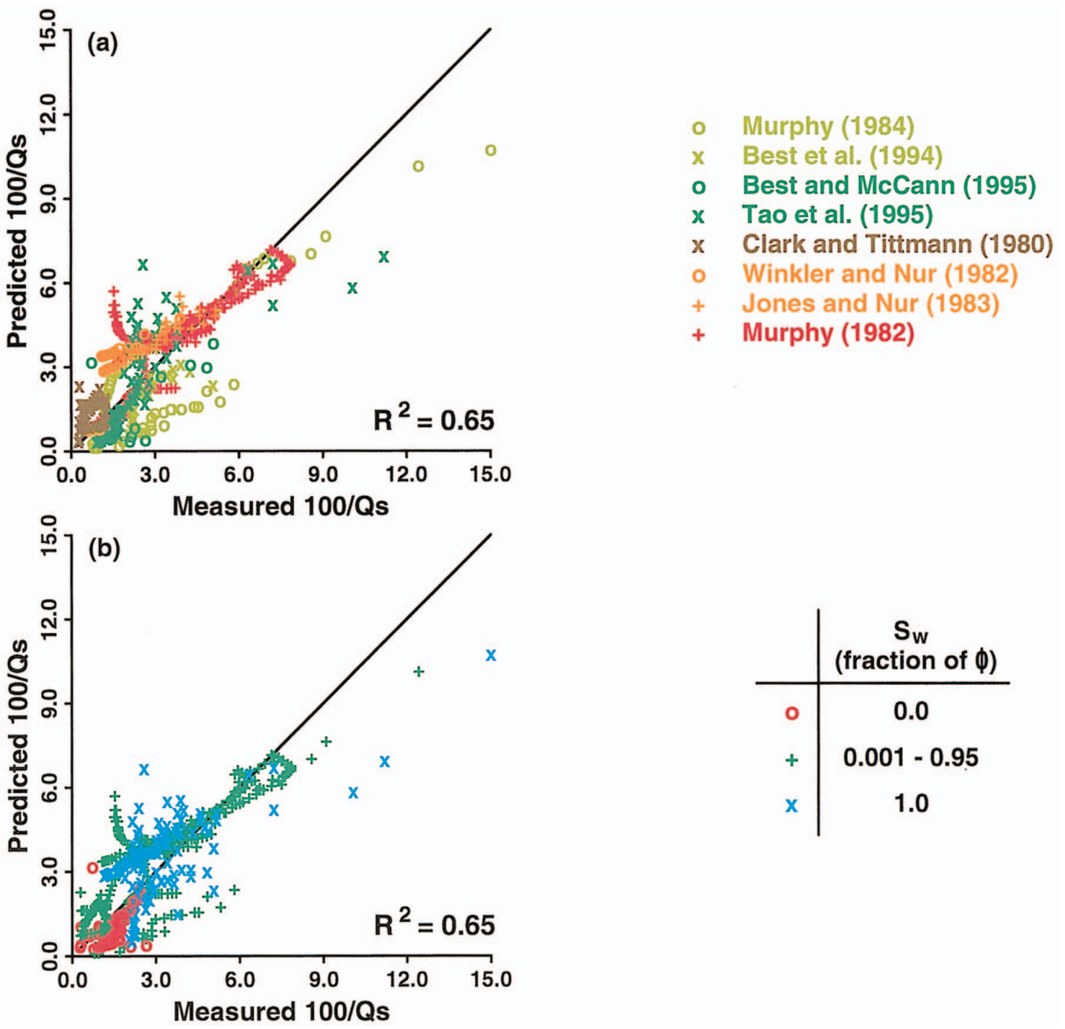

FIG. 10. Cross-plots of measured and predicted $100/Q_s$ [via predicted Q_p from equations (3) and (4), and Q_s/Q_p ratio from equation (5)]. In (a), symbols and colors show the sources of the data; in (b), colors show the ranges of saturation.

Table 7. Least-squares regression coefficients of equation (5) for Q_s/Q_p.[≤]

S_w (fraction of ϕ)	c_1	c_2	c_3	c_4	c_5	c_6
$S_{\omega,\mathrm{PA}}$ to 1.0	5.382 (0.359)	2.104 (0.251)	—	—	≥4.979 (0.343)	—
0.001 to $S_{\omega,\mathrm{PA}} \geq 0.1$	≥0.868 (0.380)	2.104	—	—	0.533 (0.207)	0.494 (0.104)
0.00 to 0.001 $f \geq 0.0125 MHz$	0.772 (0.021)	—	—	≥0.150 (0.009)	—	—
0.00 to 0.001 $f \geq 0.55 MHz$	2.752 (0.414)	—	≥0.364 (0.093)	≥0.275 (0.129)	—	—

[≤]Values in brackets are the associated standard errors. $S_{w,PA}$ is water saturation at the locus of peak Q_p (the line A-B in Figure 5). A dash (—) indicates that the corresponding variable is not significant, and so was not included in the fitting. Values between $S_{w,PA}$ and $S_{w,PA} \geq 0.1$ are obtained by linear interpolation between $S_{w,PA}$ and $S_{w,PA} \geq 0.1$ along lines of constant frequency. For $0.0 \geq S_w \geq 0.001$, values of Q_s/Q_p at $0.0125 \geq f \geq 0.55$ MHz are obtained by linear interpolation between the values at $f = 0.0125$ MHz and $f = 0.55$ MHz.

Table 8. Correlation coefficients (R^2) between measured and predicted values of V_p, V_s, V_p/V_s, ϕ, $100/Q_p$, and $100/Q_s$.[≤]

S_w (fraction of ϕ)		V_p	V_s	V_p/V_s	ϕ	$100/Q_p$	$100/Q_s$	Q_s/Q_p
0.00	R^2	0.69	0.68	—	—	—	—	0.50
	ϕ	0.389	0.248	—	—	—	—	0.477
0.002–0.98	R^2	0.92	0.90	—	—	—	—	—
	ϕ	0.367	0.233	—	—	—	—	—
0.0–0.95	R^2	—	—	—	—	—	—	0.45
	ϕ	—	—	—	—	—	—	0.204
0.0–0.98	R^2	—	—	0.70	—	—	—	—
	ϕ	—	—	0.070	—	—	—	—
1.00	R^2	0.82	0.78	0.42	—	—	—	0.12
	ϕ	0.240	0.210	0.093	—	—	—	0.206
0.00–1.00	R^2	0.90	0.85	0.68	0.86	0.88	0.65	0.72
	ϕ	0.298	0.220	0.082	0.057	1.012	1.177	0.259

[≤]The ϕ are the standard deviations of the predictions from the measurements; units of ϕ are km/s for V_p and V_s, g/cm^3 for ϕ, and the rest are dimensionless.

Gregory, A. R., 1976, Fluid saturation effects on dynamic elastic properties of sedimentary rocks: Geophysics, **41**, 895–921.

——— 1977, Aspects of rock physics from laboratory and log data that are important to seismic interpretation, *in* Payton, C. E., Ed., Seismic stratigraphy—Applications to hydrocarbon exploration: Am. Soc. Petrol. Geol. Memoir **26**, 15–46.

Han, D., Nur, A., and Morgan, D., 1986, Effect of porosity and clay content on wave velocities in sandstones: Geophysics, **51**, 2093–2107.

Johnston, D. H., 1981, Attenuation: A state-of-the-art summary, *in* Toksöz, N. M., and Johnston, D. H., Eds., Seismic wave attenuation: Soc. Expl. Geophys., Geophysics Reprint Series, **2**, 123–135.

Jones, S. M., 1995, Velocities and quality factors of sedimentary rocks at low and high effective pressures: Geophys. J. Internat., **123**, 774–780.

Jones, T. D., 1986, Pore fluids and frequency-dependent wave propagation in rocks: Geophysics, **51**, 1939–1953.

Jones, T., and Nur A., 1983, Velocity and attenuation in sandstone at elevated temperatures and pressures: Geophys. Res. Lett., **10**, 140–143.

Klimentos, T., 1991, The effects of porosity-permeability-clay content on the velocity of compressional waves: Geophysics, **56**, 1930–1939.

——— 1995, Attenuation of *P*- and *S*- waves as a method of distinguishing gas and condensate from oil and water: Geophysics, **60**, 447–458.

Klimentos, T., and McCann, C., 1990, Relationships among compressional wave attenuation, porosity, clay content, and permeability in sandstones: Geophysics, **55**, 998–1014.

Kowalis, B. J., Jones, L. E. A., and Wang H. F., 1984, Velocity-porosity-clay content systematics of poorly consolidated sandstones: J. Geophys. Res., **89**, 10 355–10 364.

Martinez, R. D., 1992, Wave propagation effects on amplitude variation with offset measurement: A modeling study: Geophysics, **58**, 534–543.

Miller, S. L. M., and Stewart R. R., 1990, Effects of lithology, porosity and shaliness on *P*- and *S*- wave velocities from sonic logs: Can. J. Expl. Geophys., **26**, 94–103.

Murphy, W. F., 1982, Effects of partial water saturation on attenuation in Massilon sandstone and Vycor porous glass: J. Acoust. Soc. Am., **71**, 1458–1468.

——— 1984, Acoustic measures of partial gas saturation in tight sandstones: J. Geophys. Res., **89**, 259–269.

Murphy, W. F., Reischer, A., and Hsu, K., 1993, Modulus decomposition of compressional and shear velocities in sand bodies: Geophysics, **58**, 227– 239.

Peselnick, L., and Outerbridge, W. F., 1961, Internal friction and rigidity modulus of Solenhofen limestone over a wide frequency range: U.S. Geol. Surv. Prof. Pap. 400B.

Raymer, L. L., Hunt, E. R., and Gardner, J. S., 1980, An improved sonic transit time-to-porosity transform: 21st Ann. Log. Symp., Soc. Prof. Well Log Analysis, Paper P.

Sams, M. S., Neep, J. P., Worthington, M. H., and King, M. S., 1997. The measurement of velocity dispersion and frequency-dependent intrinsic attenuation in sedimentary rocks: Geophysics, **62**, 1456–1464.

Schön, J. H., 1995, Physical properties of rocks: Fundamentals and principles of petrophysics, *in* Helbig, K., and Treitel S. Eds., Seismic exploration: Elsevier Science Publ Co., Inc.

Shatilo, A. P., Sondergeld, C., and Rai, C. S., 1998. Ultrasonic attenuation in Glenn Pool rocks, northeastern Oklahoma: Geophysics, **63**, 465–478.

Spencer, J. W., 1979. Bulk and shear attenuation in Berea sandstone: The effects of pore fluid: J. Geophys. Res., **84**, 7521–7523.

——— 1981. Stress relaxations at low frequencies in fluid-saturated rocks: Attenuation and modulus dispersion: J. Geophys. Res., **86**, 1803–1812.

Stoll, R. D., 1981, Acoustic waves in saturated sediments, *in* Toksöz, N. M., and Johnston, D. H., Eds., Seismic wave attenuation: Soc. Expl. Geophys. Geophysics Reprint Series **2**, 164–184.

Tao, G., King, M. S., and Nabi-Bidhendi, M., 1995, Ultrasonic wave propagation in dry and brine-saturated sandstones as a function of effective stress: Laboratory measurements and modeling: Geophysics, **43**, 299–327.

Toksöz, N. M., and Johnston, D. H., 1981. Attenuation mechanisms, *in* Toksöz, N. M., and Johnston, D. H., Eds., Seismic wave attenuation: Soc. Expl. Geophys. Geophysics Reprint Series **2**, 136–139.

Tosaya, C. A., 1982, Acoustical properties of clay-bearing rocks: PhD thesis, Stanford Univ.

Tutuncu, A. N., Podio, A. L., and Sharma, M. M., 1994, An experimental investigation of factors influencing compressional- and shear-wave velocities and attenuations in tight gas sandstone: Geophysics, **59**, 77–86.

Vernik, L., 1997, Predicting porosity from acoustic velocities in siliclastics: A new look: Geophysics, **62**, 118–128.

Wang, Z., and Nur, A., 1988, Effect of temperature on wave velocities in sands and sandstones with heavy hydrocarbons: SPE Reservoir Engineering, **3**, 158–164.

——— 1992, Elastic wave velocities in porous media: A theoretical recipe, *in* Wang, Z., and Nur, A., Eds., Seismic and acoustic velocities in reservoir rocks,v.2, Theoretical and model studies: Soc. Expl. Geophys. Geophysics Reprint Series **10**, 1–35.

Winkler, K., 1985, Dispersion analysis of velocity and attenuation in Berea sandstone: J. Geophys. Res., **90**, 6793–6800.

——— 1986, Estimates of velocity dispersion between seismic and ultrasonic frequencies: Geophysics, **51**, 183–189.

Winkler, K., and Nur, A., 1979, Pore fluids and seismic attenuation in rocks: Geophys. Res. Lett., **6**, 1–4.

——— 1982, Seismic attenuation: Pore fluids and frictional sliding: Geophysics, **47**, 1–15.

Wyllie, M. R., Gregory, A. R., and Gardner, G. H. F., 1956, Elastic wave velocities in heterogeneous and porous media: Geophysics, **21**, 41–70.